From Classical to Quantum Saturation in the Nuclear Gluon Distribution[⋆]

D.N. Triantafyllopoulos[a]

SPhT/Saclay/CEA, 91191 Gif sur Yvette, France

14 February 2005

Abstract. We study the gluon content of a large nucleus (i) in the semi-classical McLerran-Venugopalan model and (ii) in the high energy limit as given by the quantum evolution of the Color Glass Condensate. We give a simple and qualitative description of the Cronin effect and high-p_T suppression in proton-nucleus collisions.

PACS. 11.10.Hi – 12.38.-t – 13.85.Lg – 24.85.+p

1 Introduction

At high energies and/or for large atomic number A, the wavefunction of a hadron is expected to be dominated by a high density gluonic system. Gluons having occupation numbers φ of order $1/\alpha_s$, which is the maximal density allowed by their mutual interactions, overlap in phase space and saturate [1,2]. A strong classical field is associated with the wavefunction and assumes a value $\mathcal{A} \sim \sqrt{a^\dagger a} \sim \sqrt{\varphi} \sim 1/g$ at saturation. At the same time scattering amplitudes become of order 1 and unitarity limits are reached [3]. The problem can be attacked by weak coupling methods, since the non-linear phenomena "push" gluons to occupy higher momenta, and the saturation momentum Q_s, which is defined as the scale where $\varphi(Q_s) \sim 1/\alpha_s$, is a hard scale increasing as a power of energy in the small Bjorken-x limit.

Presumably one of the most complete and modern approaches to saturation is the effective theory of the Color Glass Condensate (CGC) [4,5]. Fast moving partons have a large lifetime due to time dilation and act as "frozen" sources ρ for the virtual emission of softer gluons. One solves the classical Yang-Mills equations to obtain the color field $\mathcal{A}(\rho)$ and then an observable $O(\mathcal{A})$ is determined by averaging over the possible color sources, with a probability distribution $W_Y[\rho]$. Increasing the rapidity $Y = \ln(1/x)$, more gluons need to be included in the source, and a resummation of $\alpha_s Y$ enhanced terms in the presence of a background field leads to a functional Renormalization Group Equation (RGE) for $W_Y[\rho]$ [4–7]. This RGE gives an infinite hierarchy of non-linear coupled equations, the so-called Balitsky equations [8]. The

first one describes the evolution of the scattering amplitude $\langle T_{xy} \rangle_Y$ of a color dipole $(\boldsymbol{x}, \boldsymbol{y})$ off the CGC and reads

$$\frac{\partial \langle T_{xy} \rangle_Y}{\partial Y} = \frac{\bar{\alpha}_s}{2\pi} \int d^2 \boldsymbol{z} \, \frac{(\boldsymbol{x} - \boldsymbol{y})^2}{(\boldsymbol{x} - \boldsymbol{z})^2 (\boldsymbol{z} - \boldsymbol{y})^2}$$
$$\times \langle T_{xz} + T_{zy} - T_{xy} - T_{xz} T_{zy} \rangle_Y \,, \quad (1)$$

with $\bar{\alpha}_s = \alpha_s N_c/\pi$. The first three terms correspond to the BFKL equation [9] in coordinate space [10], while the last one accounts for unitarization effects. Eq. (1) can be closed by a mean field approximation, that is by allowing the last term to factorize[1], something which should be reasonable assuming that the target is a large ($A \gg 1$) nucleus [15].

2 Classical Saturation

Classical saturation, where there is no small-x evolution, can be realized only in a large nucleus. The $A \times N_c$ valence quarks are the sources for the emission of gluons, and in the McLerran-Venugopalan (MV) model [2] they are assumed to be uncorrelated for transverse separations $\Delta \boldsymbol{x} \lesssim \Lambda_{\text{QCD}}^{-1}$, so that the probability distribution is given by the Gaussian [2,16]

$$W_{\text{MV}}[\rho] \propto \exp \left[-\frac{1}{2} \int^{1/\Lambda} d^2 \boldsymbol{x} \, \frac{\rho_a(\boldsymbol{x}) \rho_a(\boldsymbol{x})}{\mu_A^2} \right], \quad (2)$$

where $\mu_A^2 = 2\alpha_s A/R_A^2 \sim A^{1/3} \Lambda^2$ is the color charge density squared, with R_A the nuclear radius. Even though the sources are uncorrelated, the created field $\mathcal{A}$ is obtained from a non-linear equation. Thus, starting from its canonical definition, the gluon occupation number φ_A is

---

[a] *E-mail address:* dionysis@dsm-mail.saclay.cea.fr

[1] However, this factorization is not valid in the region where the amplitude is very small, namely when $T \lesssim \alpha_s^2$ [11–14].
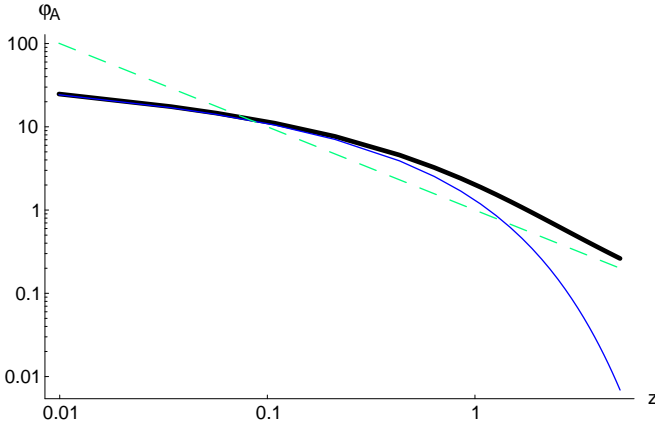
Fig. 1. *The gluon occupation number in the MV model. Thick (black), solid (blue) and dashed (green) lines show the total, CGC and BS quantities respectively.*

Fig. 2. *The integrated gluon distribution in the MV model. Thick (black), solid (blue) and dashed (green) lines show the total, CGC and BS quantities respectively.*

not the one that we would obtain from a simple superposition of the sources. When $A \gg 1$, the density can be high, sets the magnitude of the saturation scale as $Q_s^2(A) \approx \Lambda^2 A^{1/3} \ln A \gg \Lambda^2$, and we find [17]

$$\varphi_A = \frac{1}{\alpha_s} \Gamma(0, z) + \varphi_A^{\text{twist}}(z), \qquad z \equiv k^2/Q_s^2(A), \quad (3)$$

with $\boldsymbol{k}$ the transverse gluon momentum and k its magnitude. Here, Γ is the incomplete Gamma function, while the explicit expression for φ_A^{twist} can be found in [17].

The first term, enhanced by $1/\alpha_s$, dominates for all $z \lesssim 1$, as shown in Fig. 1. We interpret this compact distribution, falling exponentially at large z, as the occupation number in the CGC phase. The twist term[2] contains the bremsstrahlung spectrum (BS) $\varphi_{\text{BS}} \sim 1/z$, and is important for the large-z behavior, while it remains finite as $z \to 0$. Due to the lack of correlations among the valence quarks, a sum rule exists [2, 17–19]

$$\int^Z \mathrm{d}z \, [\varphi_A(z) - \varphi_{\text{BS}}(z)] \xrightarrow[Z \to \infty]{} 0; \quad (4)$$

the integrated distribution is obtained by "summing" over the nucleons when $Q^2 \equiv Z Q_s^2(A) \gg Q_s^2(A)$ (see Fig. 2). Thus, the effect of the repulsive interactions in the nucleus is just a redistribution of the gluons in momenta. The spectra φ_A and φ_{BS} become equal at a scale $Q_c(A)$ such that $\Lambda^2 \ll Q_c^2(A) \approx \alpha_s Q_s^2(A) \ll Q_s^2(A)$ and "infrared" gluons in excess in the BS spectrum are located at $k \sim Q_s(A)$ in the MV model. Therefore, *the MV spectrum is enhanced around the saturation scale*, as shown in Fig. 1.

As an immediate consequence, let us consider the Cronin ratio

$$\mathcal{R}_{\text{pA}} \equiv \frac{\varphi_A}{A^{1/3}\varphi_p} = \frac{\varphi_A}{\varphi_{\text{BS}}} = z \varphi_A, \quad (5)$$

with φ_p the spectrum of the proton, when this is obtained from a simple superposition of the gluons emitted by its valence quarks. It behaves as

- $\mathcal{R}_{\text{pA}} \ll 1$ if $z \ll 1$
- $\mathcal{R}_{\text{pA}} \sim \mathcal{O}(1/\alpha_s) \gg 1$ if $z \sim 1$ (6)
- $\mathcal{R}_{\text{pA}} \to 1^+$ if $z \gg 1$.

The ratio, shown in Fig. 3, has a maximum at $z_m = 0.435 + \mathcal{O}(\alpha_s)$ [17]. The maximal value $\mathcal{R}_{\text{pA}}^{\text{max}} = 0.281/\alpha_s + \mathcal{O}(\text{const})$ corresponds to a pronounced peak [17, 18, 20] originating from the compact nature of the nuclear wavefunction at saturation. This value increases with A (since $1/\alpha_s \equiv \ln Q_s^2(A)/\Lambda^2$).

3 Quantum Saturation

Now consider the evolution of a hadron to higher energies. Its wavefunction contains more and more soft gluons, due to the $\alpha_s Y$ increase in the available longitudinal phase

Fig. 3. *The Cronin ratio in the MV model. Thick (black), solid (blue) and dotted (red) lines show the total, CGC and twist contributions respectively.*

---

[2] The coefficient in front of this term is $\{\alpha_s \ln[Q_s^2(A)/\Lambda^2]\}^{-1}$, which is assumed to be equal to one. In fact, in a running coupling treatment of the problem, this identification becomes natural [17].
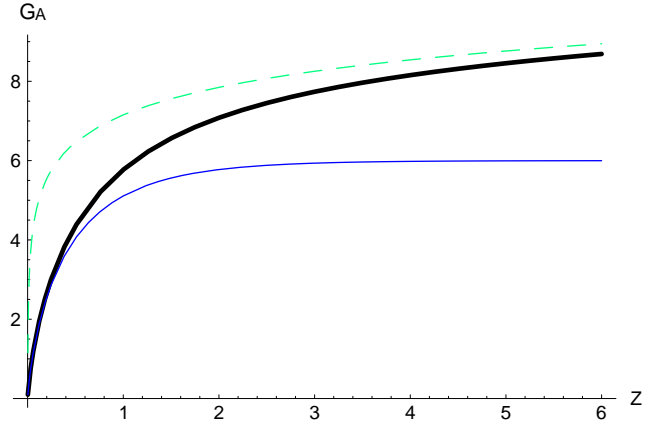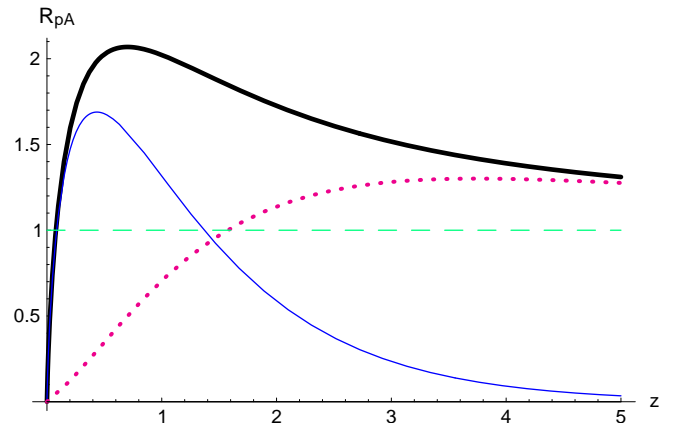
space, and correlations among the color sources are induced. The gluon occupation number may be obtained from the (averaged over impact parameter) dipole-hadron scattering amplitude as

$$\varphi(\boldsymbol{k}, Y) = \frac{1}{\alpha_s} \int \frac{\mathrm{d}^2\boldsymbol{r}}{\pi \boldsymbol{r}^2} \exp(-i\boldsymbol{k}\cdot\boldsymbol{r}) \, T(\boldsymbol{r}, Y), \qquad (7)$$

where $\boldsymbol{r}$ is the dipole size. In general, one is not able to solve Eq. (1) analytically. Only a "piecewise" expression for $\alpha_s Y \gtrsim 1$ is known, and when translated to φ it reads

$$\varphi(k,Y) = \begin{cases} \dfrac{1}{\alpha_s} \ln \dfrac{Q_s^2}{k^2} & \text{if } k \ll Q_s \\[2mm] \dfrac{1}{\alpha_s} \left(\dfrac{Q_s^2}{k^2}\right)^{\gamma_s} \left(\ln \dfrac{k^2}{Q_s^2} + \Delta\right) & \text{if } k \gtrsim Q_s \\[2mm] \dfrac{Q_0^2}{k^2} \, \mathrm{I}_0 \left(\sqrt{4\bar{\alpha}_s Y \ln \dfrac{k^2}{Q_0^2}}\right) & \text{if } k \gg Q_s, \end{cases} \qquad (8)$$

where the dominant behavior of the saturation momentum is $Q_s^2(Y) = \# Q_s^2(0) \exp[\bar{\alpha}_s \chi(\gamma_s) Y/\gamma_s]$, with $\chi(\gamma)$ the eigenvalue of the BFKL equation and $\gamma_s = 0.628$ the associated anomalous dimension [1, 21–24]. In Eq. (8), Δ is an undetermined constant and I_0 is a modified Bessel function of the first kind. From the first two pieces in this equation, it is obvious that the solution exhibits geometrical scaling [21–27] below and in a certain wide region above Q_s; it depends on k and Y only through the combination $k^2/Q_s^2(Y)$. It is instructive to do a first step in the non-linear evolution, valid so long as $Y \ll 1/\alpha_s$. To the order of accuracy and for momenta $k \lesssim Q_s(A, Y)$, it is enough to evolve only the compact piece in Eq. (3) which will add a correction of order Y. This correction contains power-law tails which are generated from the tails of the evolution kernel. It is clear that, when $Y \gtrsim 1/\alpha_s$ all the components will be "mixed" and, unlike the classical case, *in the quantum case there is no compact distribution for $k \lesssim Q_s(Y)$ and no parametric separation between the solutions above and below $Q_s(Y)$*, as can be seen in Eq. (8).

The analysis of the Cronin ratio is not trivial since we do not know the solution in the whole k-Y plane. Furthermore, given a "point" in this plane, the proton and the nucleus can be in different phases, e.g. the nucleus could be saturated while the proton is still dilute. However, we can understand the generic important features.

• The proton is "less saturated" than the nucleus, since the initial proton scale $\sim \Lambda^2$ is much smaller than the initial nuclear one $Q_s^2(A)$, and therefore the available transverse space for the proton is larger. Thus, *the proton evolves faster than the nucleus and the ratio $\mathcal{R}_{\mathrm{pA}}$ decreases*. For example, along the particular line $k = Q_s(A, Y)$, one has

$$\frac{\mathrm{d}\mathcal{R}_{\mathrm{pA}}}{\mathrm{d}Y} < 0 \quad \& \quad \mathcal{R}_{\mathrm{pA}} \xrightarrow[Y \to \infty]{} (\alpha_s A^{-1/3})^{1-\gamma_s}. \qquad (9)$$

• For fixed Y and for extremely high momenta both systems are dilute, described by the solution in the double logarithmic approximation (the last piece in Eq. (8)), and
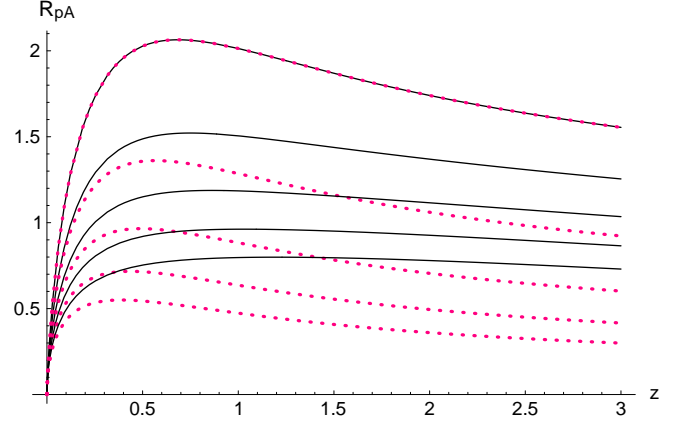

Fig. 4. *From top to bottom, the Cronin ratio for* $Y = 0, 1/2, ..., 2$, *below and near the saturation scale. Solid (black) lines correspond to an evolved nuclear wavefunction and dotted (red) to an unevolved one.*

the above mentioned difference in transverse space is now unimportant. The ratio approaches 1 from *below*, namely

$$\frac{\mathrm{d}\mathcal{R}_{\mathrm{pA}}}{\mathrm{d}k^2}\bigg|_{k^2 \gg Q_s^2(A,Y)} > 0 \quad \& \quad \mathcal{R}_{\mathrm{pA}} \xrightarrow[k^2 \to \infty]{} 1^-. \qquad (10)$$

• The sum rule breaks down for any $Y > 0$ because of the correlations induced among the sources. The peak remains for a while, since *the sum rule is a sufficient but not a necessary condition for the existence of a peak.*

• One can follow analytically the evolution of the peak, as shown in Fig. 4, until it becomes of order 1, since this happens very fast due (again) to the large separation between the scales Λ^2 and $Q_s^2(A)$. The nuclear wavefunction is almost unevolved, while the proton is still dilute. One finds

$$\mathcal{R}_{\mathrm{pA}}^{\max} = \mathcal{O}(1) \quad \text{when} \quad Y = (1/4)\ln^2(1/\alpha_s) \ll 1/\alpha_s. \qquad (11)$$

• Even though smaller than 1, a peak persists under further evolution until $Y \sim 1/\alpha_s$, when the power-law tails will have "washed-out" the compact piece in the nuclear wavefunction; *the peak flattens out due to the nuclear evolution* and the ratio becomes a monotonic function of k^2, that is

$$\frac{\mathrm{d}\mathcal{R}_{\mathrm{pA}}}{\mathrm{d}k^2} > 0 \quad \text{when} \quad Y \gtrsim 1/\alpha_s. \qquad (12)$$

These features of saturation and the Cronin ratio [17] extend previous discussions [19, 28], agree with the results obtained in numerical solutions [29], and remain qualitatively unaltered under a running coupling treatment [17].

4 Epilogue

Saturation phenomena can play a significant role in determining the produced particle spectra in high-energy heavy ion collisions. In d-Au collisions at RHIC at BNL, final state interactions are not important, and with p_{T} and η the transverse momentum and the (pseudo)rapidity of
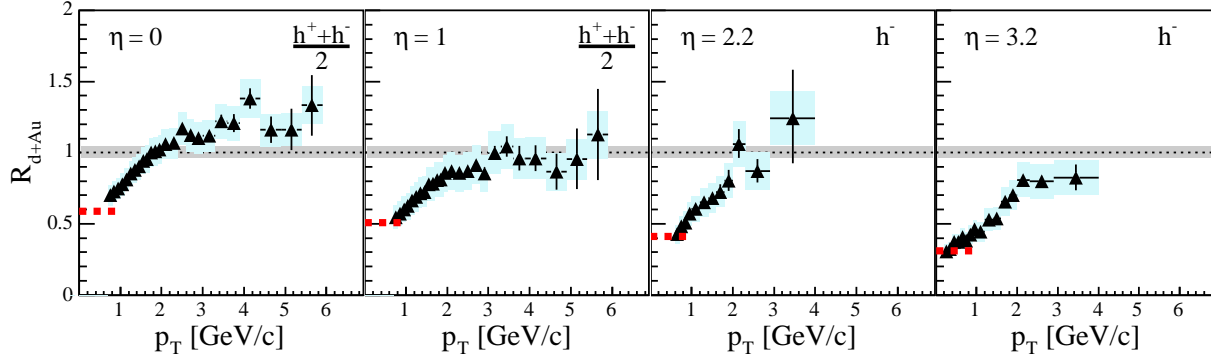
Fig. 5. *The BRAHMS data [30]: Nuclear modification factor for charged hadrons.*

the produced particle, one probes the nuclear wavefunction at a value $x_{\mathrm{Au}} \simeq 2|p_{\mathrm{T}}|\exp[-\eta]/\sqrt{s_{\mathrm{NN}}}$, where $\sqrt{s_{\mathrm{NN}}}$ is the center of mass energy per nucleon. At current energies one expects to reveal classical saturation properties in the mid-rapidity region, while quantum saturation should be realized in the forward one. Indeed, the CGC predictions (and postdictions) seem to be in reasonable qualitative agreement with the RHIC data [30] shown in Fig. 5. One should keep in mind that the gluon occupation number and the particular ratio we studied are not directly measurable quantities, and therefore any conclusion drawn at the quantitative level might be misleading. Nevertheless, more "refined" quantities like, for example, the gluon production [19, 29, 31] (and the corresponding ratio) and even the charged hadron production [32], are directly related to the gluon occupation number and share the same features as those presented in the previous sections. It could be very well the case that the data for the nuclear modification factor shown in Fig. 5 correspond to a manifestation of saturation in the nuclear wavefunction.

Acknowledgements

References

1. L.V. Gribov, E.M. Levin and M.G. Ryskin, Phys. Rep. **100** (1983) 1.
2. L. McLerran and R. Venugopalan, Phys. Rev. D **49** (1994) 2233; *ibid.* **49** (1994) 3352; *ibid.* **50** (1994) 2225.
3. A. H. Mueller, Nucl. Phys. B **437** (1995) 107.
4. E. Iancu, A. Leonidov and L. McLerran, Nucl. Phys. A **692** (2001) 583; Phys. Lett. B **510** (2001) 133.
5. E. Ferreiro, E. Iancu, A. Leonidov and L. McLerran, Nucl. Phys. A **703** (2002) 489.
6. H. Weigert, Nucl. Phys. A **703** (2002) 823.
7. J. Jalilian-Marian, A. Kovner, A. Leonidov and H. Weigert, Nucl. Phys. B **504** (1997) 415; Phys. Rev. D **59** (1999) 014014.
8. I. Balitsky, Nucl. Phys. B **463** (1996) 99; Phys. Rev. Lett. **81** (1998) 2024; Phys. Lett. B **518** (2001) 235.
9. L.N. Lipatov, Sov. J. Nucl. Phys. **23** (1976) 338; E.A. Kuraev, L.N. Lipatov and V.S. Fadin, Sov. Phys. JETP **45** (1977) 199; Ya.Ya. Balitsky and L.N. Lipatov, Sov. J. Nucl. Phys. **28** (1978) 822.
10. A.H. Mueller, Nucl. Phys. B **415** (1994) 373.
11. A.H. Mueller and A. Shoshi, Nucl. Phys. B **692** (2004) 175.
12. E. Iancu, A.H. Mueller and S. Munier, Phys. Lett. B **606** (2005) 342.
13. E. Iancu and D.N. Triantafyllopoulos, arXiv:hep-ph/0411405; hep-ph/0501193.
14. A.H. Mueller, A. Shoshi and S.M.H. Wong, arXiv:hep-ph/0501088.
15. Yu.V. Kovchegov, Phys. Rev. D **60** (1999) 034008.
16. Yu.V. Kovchegov, Phys. Rev. D **54** (1996) 5463.
17. E. Iancu, K. Itakura and D.N. Triantafyllopoulos, Nucl. Phys. A **742** (2004) 182.
18. F. Gelis and A. Peshier, Nucl. Phys. A **697** (2002) 879.
19. D. Kharzeev, Yu.V. Kovchegov and K. Tuchin, Phys. Rev. D **68** (2003) 094013.
20. F. Gelis and J. Jalilian-Marian, Phys. Rev. D **67** (2003) 074019.
21. E. Iancu, K. Itakura and L. McLerran, Nucl. Phys. A **708** (2002) 327.
22. A.H. Mueller and D.N. Triantafyllopoulos, Nucl. Phys. B **640** (2002) 331.
23. D.N. Triantafyllopoulos, Nucl. Phys. B **648** (2003) 293.
24. S. Munier and R. Peschanski, Phys. Rev. Lett. **91** (2003) 232001; Phys. Rev. D **69** (2004) 034008.
25. K. Golec-Biernat, J. Kwieciński and A.M. Staśto, Phys. Rev. Lett. **86** (2001) 596.
26. M. Lublinsky, Eur. Phys. J. C **21** (2001) 513.
27. K. Rummukainen and H. Weigert, Nucl. Phys. A **739** (2004) 183.
28. D. Kharzeev, E. Levin and L. McLerran, Phys. Lett. B **561** (2003) 93.
29. J. Albacete, N. Armesto, A. Kovner, C.A. Salgado and U.A. Wiedemann, Phys. Rev. Lett. **92** (2004) 082001.
30. I. Arsene *et al.* (BRAHMS Collaboration), Phys. Rev. Lett. **93** (2004) 242303.
31. J.-P. Blaizot, F. Gelis and R. Venugopalan, Nucl. Phys. A **743** (2004) 13; *ibid.* **743** (2004) 57.
32. D. Kharzeev, Yu.V. Kovchegov and K. Tuchin, Phys. Lett. B **599** (2004) 23.